NASA TECHNICAL MEMORANDUM

NASA TM X-52942

NASA TM X-52942

LUBRICATION CONSIDERATIONS IN GEAR DESIGN

by D. P. Townsend
Lewis Research Center
Cleveland, Ohio

TECHNICAL PAPER proposed for presentation at
Gear Seminar "Operation Update" sponsored by
the American Society of Mechanical Engineers
Cleveland, Ohio, December 10, 1970

LUBRICATION CONSIDERATIONS IN GEAR DESIGN

by Dennis P. Townsend

Lewis Research Center
National Aeronautics and Space Administration
Cleveland, Ohio

E-6094

ABSTRACT

Mechanical and service variables must be considered to obtain optimum gear performance under severe operating conditions. The lubricant in gearing prevents failure under several regimes of operation, such as boundary lubrication, mixed lubrication, and full elastohydrodynamic (EHD) film operation. Gears operating under boundary and mixed lubrication require added protection by using extreme pressure (EP) and antiwear additives to prevent failure. Understanding the mechanism of how these additives work can aid the designer in his selection of a lubricant for a particular application. In many applications gears operate with a full EHD film. The method of EHD film formation and how the lubricant properties affect the film will be presented and discussed. An analytical method for determining EHD film thickness from theory and how the film affects gear failure mode and life will be presented.

NOMENCLATURE

b	Hertzian half width, in.
C	center distance, in.
D_o	outside diameter of gear, in.
d_o	outside diameter of pinion, in.
D_b	base diameter of gear, in.
d_b	base diameter of pinion, in.
E	elastic modulus, lb/in.^{2}
E'	equivalent elastic modulus, lb/in.^{2}
e	exponent, 2.718
G	$\alpha E'$ dimensionless material parameter
H_{min}	h/R dimensionless film parameter
h_{min}	EHD film thickness, inches or microinches
n	exponent of h for fatigue life
P	pressure in contact zone, lb/in.^{2}
$R_{1,2}$	radius of contacting rollers, in.
R	equivalent radius, in.
$U_{1,2}$	tangential velocity of rolling contact, in/sec.
U	$= \mu_o (U_1 + U_2) E' R$ dimensionless speed parameter
W	$= w'/E'R$ dimensionless load parameter
W'	load per unit with, lb/in.
X	distance along the line of action, in.
Z	length of line of action, in.
α	pressure viscosity coefficient, in^2/lb.
δ	poisson ratio
Λ	EHD film to roughness parameter

μ_o	lubricant viscosity at atmospheric pressure, lb. sec/in.^{2}
μ	lubricant viscosity at contact pressure, lb. sec/in.^{2}
ν	lubricant viscosities, centistokes
ρ	density, gram/cc
σ	composite surface roughness, rms
$\sigma_{1,2}$	surface roughness of contacting surfaces, rms
ψ	gear pressure angle, degrees
ω	rotational speed, radians/sec.

INTRODUCTION TO GEAR LUBRICATION

The lubrication of gears and bearings involves a complex technology which includes such things as fluid film thickness, thermal considerations, chemistry of additives, and lubricant properties such as viscosity. Gears are subject to several types of failure modes, as shown in Figure 1 (Reference 1). From this figure it can be seen that gears can fail by wear at low speed and high loads or by scoring or pitting at high loads over a wide speed range.

With the present state of gear design the predominate mode of failure in gears that must operate at high speed and transmit high loads is scoring. Basically, scoring can be described as the result of a breakdown in the lubricant and/or boundary film separating the load carrying members. Therefore, the main function of the gear lubricant is to prevent the gears from scoring at the operating load and speed required. This is accomplished by the lubricant in two distinct ways: (1) by providing an unbroken film of lubricant between the teeth or load-carrying members, and (2) by cooling the gear so that the film of lubricant does not become too thin or broken.

There are many factors that can affect the start of scoring. Some of these factors which affect scoring are shown in Figures 2 to 4 (Reference 2). Figure 2 shows the effect of surface finish on scoring where the load capacity at 20 microinches rms is approximately twice the load capacity at 60 microinches rms. For the example shown, increased surface roughness above about 60 microinches rms does not seem to reduce load-carrying capacity appreciably. Others have shown similar results (Reference 3).

Figure 3 shows how tip relief can improve the scoring load capacity of a set of gears. In this case, tip relief up to 0.0008 was effective in improving load capacity, but beyond 0.0008 the load capacity was reduced. Tip relief is effective because it corrects for tooth deflection that would cause the gear teeth to contact unevenly or incorrectly. Other mechanical factors such as alignment and diametral pitch can have an effect on the scoring load. Several operating factors can also have an effect on load capacity. These are speed, temperature, and viscosity of the lubricant as well as the type of additive present in the lubricant.

A notable effect on the load-carrying capacity of gears is the method of applying the lubricant to the gear, as shown in Figure 4 (Reference 1). Here 0° represents the gears coming into mesh and 360°, the gears going out of mesh. As can be seen, the load capacity is affected by the jet velocity and by the jet location. The jet velocity can affect how much oil strikes the tooth as well as the cooling rate of the lubricant. Usually the best cooling of the gear tooth surface is obtained by jet application at the gear outlet and best lubrication at the gear inlet. It will be shown later that cooling of the gear tooth surface is very important in improving load carrying capacity.

In wide gears operating at high speeds considerable power can be lost by applying jet lubricant to the inlet mesh because the gears will trap the lubricants between the gear teeth as shown in Figure 5. In such cases, a fine mist spray or low oil flow jet would best serve to apply lubricant to the gear teeth at the inlet mesh. Mist lubrication can supply adequate lubricant to the surfaces but will not supply adequate cooling in most cases.

In jet cooling of the gear teeth, it is also important that the jet of lubricant have sufficient velocity and be in the proper direction so that it will strike the tooth surface that should be cooled, Figure 5 (Reference 4). The amount of lubricant remaining on the tooth as it approaches the inlet mesh is a function of the viscosity, which is a function of temperature; this indicates that cooling on the outlet mesh will help the lubricant film at the inlet mesh.

BOUNDARY LUBRICATION

Extreme-pressure lubricants can significantly increase the load carrying capacity of gears. The extreme-pressure additives in the lubricating fluid form a film on the surfaces by chemical reaction, adsorption, and/or chemisorption. These boundary films can be less than one microinch to several microinches thick (Reference 6). These films may appear as shown in Figure 6 (Reference 5) for the chemical reaction of sulfur and in Figure 7 for the chemisorption of iron stearate. Figure 8 shows the range of film thicknesses for various films (Reference 6). The films can provide separation of the metal surfaces when the lubricant becomes thin enough for the asperities to interact. The boundary film probably provides lubrication by microasperity-elastohydrodynamic lubrication (Reference 7), as shown in Figure 9; here the asperities deform under the load. The boundary film prevents contact of the asperities and at the same time provides low shear strength properties that prevent shearing of the metal and reduce the friction coefficient over that of the base metal. These boundary films provide lubrication at different temperature conditions, depending on the materials used. For example, some boundary films will melt at a lower temperature than others, as can be seen in Figure 10 (Reference 5), and will then fail to provide protection of the surfaces. The "failure temperature" is the temperature at which the lubricant film fails.

In extreme-pressure lubrication this failure temperature is the temperature at which the boundary film melts. The melting point or thermal stability of surface films appears to be one unifying physical property governing failure temperature for a wide range of materials (Reference 5). It is based on the observation (Reference 8) that only a film which is solid can properly interfere with potential asperity contacts. For this reason, many extreme-pressure lubricants contain more than one chemical for protection over a wide temperature range. For instance, Borsoff (References 9 and 10) found that phosphorus compounds were superior to chlorine and sulfur at slow speeds, while sulfur was superior at high speeds. He explains this as a result of the increased surface temperature at the higher speeds. It should be remembered that most extreme-pressure additives are chemically reactive and increase their chemical activity as temperature is increased. Horlick (Reference 11) found that some metals such as zinc and copper had to be removed from their systems when using certain extreme-pressure additives.

EXTREME PRESSURE AND ANTI-WEAR ADDITIVE SELECTION

Some of the extreme-pressure additives commonly used for gear oil are those containing one or more compounds of chlorine, phosphorus, sulfur or lead soaps (Reference 12). Many chlorine containing compounds have been suggested for extreme-pressure additives but few have actually been used. Some lubricants are made with chlorine containing molecules where the Cl_3-C linkage is used. For example, either tri (trichloroethyl) or tri (trichlortert butyl) phospate additives have shown high load carrying capacity. Other chlorine containing additives are chlorinated paraffin or petroleum waxes and hexachlorethene.

The phosphorus containing compounds are perhaps the most commonly used additives for gear oils. Some aircraft lubricants have 3-5% tricresyl phosphate or tributyl phosphite as either an extreme-pressure or anti-wear agent. Other phosphorus extreme-pressure agents used in percentages of 0.1 to 2.0% could be dodecyl dihydrogen phosphate, diethyl-, dibutyl-, or dicresyl- phenyl trichloroethyl phosphite and a phosphate ester containing a pentachlorphenyl radical. Most of the phosphorus compounds in gear oils also have other active elements.

The sulfur containing extreme-pressure additives are believed to form iron sulfide films that prevent wear up to very high loads and speeds. However, they give higher friction coefficients and are, therefore, usually supplemented by other boundary film forming ingredients that reduce friction. The sulfur compounds should have controlled chemical activity (such as oils containing dibenzyl disulfide of 0.1 or more percent). Other sulfur containing extreme-pressure additives are diamyl disulfide, dilauryl disulfide, sulfurized oleic acid and sperm oil mixtures, and dibutylxanthic acid disulfide.

Lead soaps have been used in lubricants for many years. They resist the wiping and sliding action in gears and they help prevent corrosion of steel in the presence of water. Some of the lead soaps used in lubricants are lead oleate, lead fishate, lead-12-hydroxystearate, and lead naphthenate. The lead soap additive most often used is lead naphthenate because of its solubility. Lead soaps are used in concentrations of from 5-percent to 30-percent.

There are other additive compounds that contain combinations of these elements and most extreme-pressure lubricants contain more than one extreme-pressure additive. Needless to say, the selection of a proper extreme-pressure additive is a complicated process. The word susceptibility is frequently used with reference to additives in oils to indicate the ability of the oil to accept the additive without deleterious effects. Such things as solubility, volatility, stability, compatibility, load carrying capacity, cost, etc., must be considered.

Many gear oil compounds depend upon the use of proprietary or package extreme-pressure additives. As a result, the lubricant manufacture does not evaluate the additives' effectiveness. Because of this, any selection of extreme-pressure additives should be supported by an evaluation program to determine their effectiveness for a given application. However, a few firms have considerable background in the manufacture and use of extreme-pressure additives for gear lubrication and their recommendations are usually accepted without question by users of gear oils.

Reference 12 lists several representative oil formulations for different applications containing several additives. Table 1 is a list of three lubricants with additives for hypoid gear operation. Table 2 is a list of four lead containing extreme-pressure gear oils. The SCL is a compound containing sulfur-chlorine-lead and fatty oil. Table 3 is a typical formulation for a jet turbine lubricant.

ELASTOHYDRODYNAMIC LUBRICATION

In elastohydrodynamic lubrication, called EHD (or EHL by the British), the contacting surfaces, even under high loads such as those obtained in gears and bearings, elastically deflect and are separated by a thin EHD film of lubricant which is a few microinches to several microinches thick. The flattening of the contact of curved surfaces elastically under load reduces the resultant contact pressure from that of pure line or point contact. Under the high contact stresses, the fluid in the contact zone tends to be squeezed out. However, as the lubricant is pressurized by the contact pressure, its viscosity increases several orders of magnitude. This increase in viscosity with pressure is shown in Figure 11 (Reference 13). In the ASME report (Reference 13), the pressure of the liquid was varied up to several thousand psi at different temperatures and the

viscosity measured by a weight falling through the fluid. The curves of Figure 11 are for a synthetic lubricant diester, di(2-ethyl-hexyl) sebacate, which is the base stock for some Mil-L-7808 lubricants. Here it can be seen that, as the fluid is subjected to pressures of 150,000 psi at 77° F, the viscosity increases from 18 centipoise at atmospheric pressure to 400,000 centipoise at 150,000 psi. The fluid at this extremely high viscosity resists being squeezed out of the contact zone, and the load is thus transmitted from one element through the lubricant film to the other element. In fact, it can be, and has been, shown that a steel ball can be loaded against a bearing groove with 200,000 psi maximum Hertz stress (that is, the maximum contact pressure) and with a lubricant film on the groove, the surfaces will remain separated for several hours. Figure 12 (Reference 14) is a cross section through the film of a ball loaded against a flat plate and shows how the pressure-viscosity effects increase the film thickness in the higher pressure region near the center of the contact zone.

Several people have measured the EHD film thickness between rolling disks and between a ball and disk by at least four different methods. Sibley et al, (Reference 15), at Battelle have measured the EHD film thickness between rolling disks using X-ray techniques. Figure 13 is a view of the X-ray disk apparatus used at Battelle. Here an X-ray source is collimated into a beam which is passed through the contact zone. A Geiger counter on the other side of the contact zone measures the intensity of the X-ray which determines the film thickness. Figure 14 is a film thickness measurement along the axial direction. Film thickness can also be taken in the circumferential direction. Battelle has also measured the film pressures and temperatures using thin film transducers on the surface of the disk.

Crook (Reference 16) first measured film thickness of the EHD oil film indirectly by measuring the capacitance between the disk at the outlet of the contact and a trailing pad which assumes the thickness measured is one-half the EHD film thickness.

Dyson (Reference 17) measured the capacitance between two disks directly to obtain the EHD film thickness. Dyson measured the film thickness of several lubricants with pure rolling and with rolling and sliding. Figure 15 is a typical curve obtained by Dyson where he compares the calculated film thickness with the measured film thickness. As can be seen, the measured film thickness compares favorably with the calculated film thickness except at the larger film thickness, where it departs slightly because it is becoming more hydrodynamic than EHD. It is interesting to note here that the film thickness with pure rolling and that with rolling and sliding are identical, which indicates that sliding may have no influence on the EHD film thickness. This is predicted by theory which says the film thickness is dependent on the inlet viscosity only. Crook has shown this, as can be seen in Figure 16 (Reference 16), where the introduction of

severe sliding at constant sum velocities and inlet viscosity reduced the viscosities in the contact zone from 600 poise to 14 poise, while the film thickness fell only 10-percent.

SKF Industries under contract to NASA has measured film thickness in bearings using the capacitance method and a method developed by SKF which could be called the conductivity method. With this method, a 400-cycle mv potential is impressed across the bearing races, and the number of asperity contacts is measured. Using the data obtained and a calibration curve obtained analytically, the film thickness can be determined over a limited range. This range is an h/σ of approximately 1.5 to 4. When the capacitance method is used, it will not measure very accurately below the film thickness where asperities began to touch since at this point it begins to short the capacitance. Below this point, which is an h/σ of approximately 4, the oonductivity method measures the film thickness. Figure 17 is a photograph of the oscilloscope trace of the conductivity method. Here one can see the 400-cycle voltage; the verticle lines or spikes on this trace are asperity contacts. This particular trace represents a film parameter h/σ of approximately 3.5.

Another one of the very interesting methods of measuring EHD film thickness is the optical method developed by Dr. A. Cameron at Imperial College, London (Reference 14). Figure 18 shows how this device works. Light is passed through a glass or other transparent material such as saphire and is reflected from the contact zone into a lens system in the form of newton rings which give a measure of the film thickness at the contact zone of the rotating ball and transparent plate. Figure 19 is a photograph of the image seen through the eyepiece. The film thickness is measured by watching the contact zone from startup and counting the number of rings as the film thickness increases. The variation in film thickness can be seen in the figure. The minimum film thickness occurs at the sides of the contact, where side leakage reduces the film thickness. The trailing edge is also somewhat thinner than the center region of the contact zone because of oil starvation and/or leakage at the contact outlet. Figure 20 is a profile in two directions of the film thickness measured by the optical method. It can be seen that the film thickness at the sides is approximately half that in the center of the contact zone, while the exit film thickness is reduced approximately 20-percent.

Although considerable research has been applied to EHD technology, there is still much to learn. Specifically, more information is needed on the properties of the fluid as it undergoes rapid changes in pressure, temperature, and shear rate. Also, a better understanding is needed on the thermal conditions existing in the films and surfaces during rolling and sliding conditions.

In order to determine the EHD film thickness by using existing theories, the temperature of the lubricants entering the contact zone must be known.

This temperature is practically identical to the temperature of the metal surface on which it lies. If this temperature of the metal is to be known, it must either be measured or calculated from the traction force in the contact zone. This traction force is not the same as a coefficient of friction because the force changes over the width of the contact zone and is dependent on the lubricant viscosity. As the contact zone undergoes sliding and increased temperatures, the viscosity changes considerably. The temperature and shear rate reduce the viscosity at pressure. If the viscosity followed an exponential increase, the lubricant would become stronger than the bearing metal.

H. Naylor (Reference 18) presented a plot of friction against sliding speed (Figure 21) to show how the friction changes with increased sliding speed and possible causes for this change. In work conducted at NASA (Reference 19) the traction in a spinning contact of a ball in a lubricated groove was measured and an analysis conducted to calculate the traction force in the spinning contact zone. In the analysis, the curve shown in Figure 22 as used with the pressure-viscosity equation as shown. When this equation was used, the analysis matched the experimental analysis, as shown in Figure 23. Tests were also conducted at NASA-Lewis Research Center (Reference 20) to determine what effect several additives would have on the traction forces in a spinning EHD contact. As can be seen from Figure 24, the effects of different concentrations of several additives in a synthetic paraffinic oil had no effect on the traction force, even with a film thickness that could be considered in the regime where asperity interaction would occur. The implications from these data are that the additive used here does not affect the traction force in the contact zone and does not change the rheological properties of the lubricant.

With some simplifying assumptions the design procedure presented here can be used to predict the EHD film thickness in the gear tooth contact or in ball or roller bearings. Because there is still much to be learned in this complex technology, component testing is still necessary to validate the analytical predictions. Even with this limitation, this method will reduce the need for extensive and expensive testing.

Elastohydrodynamic Theory

Formation of a lubricant film between rolling elements such as gears and bearings results from the elastic deformation of the surfaces and the hydrodynamic action of the lubricant. The flattening of the surfaces spreads the load and reduces the contact pressure while the viscous drag and rolling action can draw the lubricant into the contact area (Reference 21). As the lubricant enters the contact zone, it undergoes a pressure rise. The pressure rise sharply increases the lubricant viscosity to a very high value and prevents the lubricant from being squeezed from between the surfaces. The increase of viscosity with pressure is commonly represented as

$$\mu = \mu_o e^{\alpha p} \qquad (1)$$

Pressure does not affect the atmospheric viscosity μ_o nor the pressure-viscosity coefficient α.

A. N. Grubin in 1949 developed an approximate film-thickness equation for highly loaded elastic contacts which allowed for the effect of pressure on viscosity (Reference 22). The Grubin model of an EHD lubricated contact is shown in Figure 25.

Grubin's model simplifies the EHD lubrication problem by considering long cylinders and thus disregarding variations in the axial direction. Also, the model assumes that deflections of the contacting surfaces, specifically in the inlet region, are the same under elastohydrodynamic conditions as they would be in static dry contact. The solution for film thickness is thus based on a Hertzian shape for the deformed cylinders, in the inlet region, and can be expressed as:

$$\frac{h_{min}}{R} = 1.18 \left(\frac{W'}{E'R}\right)^{-1/11} \left[\frac{\mu_o \alpha (U_1 + U_2)}{R}\right]^{8/11} \qquad (2)$$

Since the inlet viscosity and the pressure viscosity coefficient are both reduced by increased temperature, it is very important to use the correct temperature of the lubricant when calculating the EHD film thickness. Since the lubricant temperature entering the contact zone is practically identical to the metal temperature regardless of the bulk of oil temperature, the metal temperature should either be measured or calculated.

A simplified dimensionless approximation of Equation 10 is

$$H_{min} = 1.18 \frac{(GU)^{8/11}}{W^{1/11}} \qquad (3)$$

where H_{min} is the dimensionless film thickness, equal to h_{min}/R; G is the materials parameter, equal to $\alpha E'$; W is the load parameter, equal to $W'/E'R$; and W' is the applied tooth load in lb. per in. of tooth width. The speed parameter U is

$$U = \mu_o (V_1 + V_2)/E'R$$

The elastic properties of an equivalent cylinder E' are

$$1/E' = 1/2 \left\{\left[(1 - \delta_1^2)/E_1\right] + \left[(1 - \delta^2)/E_2\right]\right\}$$

For typical steels, E' is $33/10^6$ and, for mineral oils, a typical value of α is $1.5/10^4$ in.^{2}/lb. Thus, for mineral-oil-lubricated rolling elements, G = 5000. From Figure 26, values of H_{min} and h_{min} can be obtained for combinations of G, U, and W.

Contact geomety of gears and cams can be represented by two contacting cylinders. The geometric similarity outside the contact zone is not of importance.

When using contacting cylinders to approximate the contact of machine elements, it is useful to introduce the concept of an equivalent cylinder.

It is assumed the undeformed cylinders are separated by a minimum film thickness h_{min} (Figure 27a). A cylinder with equivalent radius R and with the same minimum film thickness is shown in Figure 27b. The equivalent radius is

$$R = \frac{R_1 R_2}{R_1 + R_2} \tag{4}$$

If R_1 and R_2 lie on the same side of the common tangent, then

$$R = \frac{R_1 R_2}{R_1 - R_2} \tag{5}$$

The tangential velocities are

$$U_1 = \omega_1 R_1 \tag{6}$$

$$U_2 = \omega_2 R_2 \tag{7}$$

Example 1

Find the film thickness between two steel rollers 1/4-inch wide, diameters of 3 and 2-inches with a load of 500-pounds using Mil-L-7808 lubricant at 210° F. The smaller roller speed is 2000 rpm with no slip between rollers. $= 0.40 \times 10^{-4}$ in^2/lb.

use $\frac{h_{min}}{R} = 1.18 \left(\frac{W'}{E'R}\right)^{-1/11} \left(\frac{\mu_o \alpha \quad (U_1 + U_2)}{R}\right)^{8/11}$

$W' = P/L = 500/.25 = 2000$ lb/in

$\frac{1}{E'} = 1/2 \left(\frac{1-.09}{30\times10^6} + \frac{1-.09}{30\times10^6}\right)$

$E' = 33 \times 10^6$

$\nu = 3.3$ centistokes for Mil-L-7808 at 210° F

$\mu_o = \nu\rho \quad 1.45 \times 10^{-7} = 3.3 \times .915 \times 1.45 \times 10^{-7}$

$\mu_o = 4.38 \times 10^{-7}$ # sec/in^2

$R = \frac{R_1 R_2}{R_1 + R_2} = \frac{1.5 \times 1}{2.5} = 0.6$ in

$U_1 = U_2 = \frac{\pi R N}{30} = \frac{\pi \times 1 \times 2000}{30} = 210$ in/sec

$\frac{h_{min}}{R} = 1.18 \left(\frac{2000}{33\times10^6 \times .6}\right)^{-.091} \left(\frac{4.38\times10^{-7} \times .4 \times 10^{-4} \times 420}{.6}\right)^{.727}$

$h_{min}/R = 5\times10^{-6} \qquad h_{min} = 3 \times 10^{-6}$ inches

The geometry of an involute gear contact is shown in Figure 28. Contact at distance X from the pitch point can be represented by two cylinders rotating at the angular velocity of the wheels. Equivalent radius, from Equation 1, is

$$R = \frac{(R_1 \sin \psi + X)(R_2 \sin \psi - X)}{(R_1 + R_2)\sin \psi} \tag{8}$$

Contact speeds from Equation 3 are

$$U_1 = (R_1 \sin \psi + X)\omega_1 \tag{9}$$

$$U_2 = (R_2 \sin \psi - X)\omega_2 \tag{10}$$

How Thick a Film ?

Surface topography is important to the EHD lubrication process. EHD theory is based on the assumption of perfectly smooth surfaces, that is, no interaction of surface asperities. Actually, of course, this is not the case. An EHD film of several millionths of an inch can be considered adequate for highly loaded rolling elements in a high-temperature environment. However, the calculated film might be less than the combined surface roughness of the contacting elements. If this condition exists, surface asperity contact, surface distress (in the form of surface glazing and pitting), and surface smearing or deformation can occur. Extended operation under these conditions can result in high wear, excessive vibration, and seizure of mating components. A surface-roughness criterion for determining the extent of asperity contact is based upon the ratio of film thickness to a composite surface roughness. The film parameter Λ is

$$\Lambda = \frac{h_{min}}{\sigma} \tag{11}$$

where composite roughness σ is

$$\sigma = (\sigma_1 + \sigma_2)^{1/2} \tag{12}$$

and σ_1 and σ_2 are the rms roughness of the two surfaces in contact. Figure 29 is a plot, based upon experimental data, of percent of complete asperity or surface separation, percent film, as a function of film parameter Λ. At values of less than 1, surface smearing or deformation, accompanied by wear, will occur (Figure 30d). When Λ is between 1 and 1.5, surface distress such as shown in Figure 30c can occur. For values between 1.5 and 3 some surface glazing occurs (Figure 30b). At values of 3 or greater, minimal wear can be expected with the resulting surface appearance illustrated in Figure 30a. These figures are those of bearing inner races.

Contact Pressure — Different From Theory

Typical EHD pressure traces in the contact zone, theoretically obtained, are shown in Figure 31. The maximum Hertz stress (maximum contact pressure) corresponding to dry contact is shown by the semielliptical curve. For a contacting cylinder,

$$S_{max} = \frac{W^{1/2}}{\pi} E' \tag{13}$$

and

$$b = 2RW^{1/2} \tag{14}$$

where

$$W = W'/E'R$$

An unusual feature of the pressure distributions in the contact zone is the presence of a pressure spike. At low tangential velocities, the spike is near the trailing edge of the contact zone. At higher velocities, it shifts toward the leading edge, and the pressure patterns differ sharply from the Hertz dry-contact pattern.

For those cases corresponding in Figures 31a, c, and d, maximum shearing stress is about the same magnitude as for dry contact. The case shown in Figure 31b has a stress about 15-percent higher than dry contact stress. Also, for cases shown in Figure 31a and b, maximum shearing stresses occurred closer to the surface of the contact area.

Experimental work has shown that actual pressure distributions deviate from those predicted from theory. This is illustrated in Figure 32 for contacting cylindrical disks at maximum Hertz stresses between 104,000 and 128,000 psi. The pressure curve tends to warp the calculated Hertz (dry-contact) stress distribution. The pressure spike tends to move toward the trailing edge. This trend continues for higher contact stresses. However, for these higher stresses, the pressure spike cannot be experimentally detected.

What is significant about the pressure profiles is that the average Hertz stress is decreased from the nonlubricated condition. For similar pressure profiles, a 10-percent decrease in the average stress can mean a 100-percent increase in fatigue life.

Elastohydrodynamic Lubrication and Fatigue Life — Strong Relationship

When a sufficient EHD film is present, gears will have much longer lives and will usually fail from fatigue. Fatigue usually manifests itself, in the early stages, as a shallow spall with a diameter about the same as the contact width. A fatigue failure for gears is shown in Figure 33 (Reference 24). As atmospheric viscosity of a particular lubricant is increased, the fatigue life of the gear or bearing also increases.

If the lubricant pressure-viscosity coefficient is increased by changing the lubricant base stock, longer fatigue life can be obtained for a given lubricant at atmospheric conditions. It has become generally accepted that fatigue life increases with increases in viscosity, pressure-viscosity coefficient, or speed. These factors imply increasing fatigue life with increasing EHD film thickness

$$\text{Life} \propto (h_{min})^n \tag{15}$$

Much experimental work needs to be done to determine the value of the exponent n. However, it appears that an interrelation exists among fatigue life, contact-pressure distribution, and lubricant film thickness. In Reference 22 the value of n was taken to be 0.36.

How to Use EHD Theory

Using the principles and theory previously discussed, design procedures for EHD application can be outlined. It is important, however, to realize that further refinements of EHD theory are required and are currently being undertaken. It is also very important to use the correct inlet oil temperature, which usually corresponds to the metal temperature. The methods presented do not consider non-Newtonian behavior of the lubricant. This factor probably accounts for the fact that some measurements of EHD film thickness were less than half the value predicted by theory. Thus, these procedures are a guide only — not a guarantee of successful gear or bearing operation. The procedure is

1. Determine equivalent radius R, from Equation 8.
2. Determine contact speed U_1 and U_2 from Equations 9 and 10.
3. Determine values for G, U, and W from Equation 3.
4. Calculate the dimensionless film thickness H_{min} from Equation 3 or Fig. 26.
5. Determine film thickness h_{min} from Equation 2.
6. Determine surface composite roughness σ from Equation 12 and the film parameter from Equation 11.
7. With Λ, determine from Figure 7 the percent film. If the percent film is less than 80-percent, which is equivalent to a Λ of 2, changes in one or more of the EHD parameters should be considered to avoid surface distress.
8. Where Λ is less than 2 and where operating conditions or lubricant cannot be changed, to improve the Λ value, careful consideration must be taken to properly select EP or antiwear additives to assure long life operation without gross surface distress or wear.

Example 2

Find the film thickness and h/ at the end point of tooth contact for a set of steel gears running at 5000 rpm with 7808 lubricant at 210° F. Tooth load is 2000 lb/in at all points of contact. Pitch diameter 3.5-inches, outside diameter 3.75-inches, diametral pitch 8 and surface finish 12 microinches rms.

$$Z = \frac{\left[D_o^2 - D_b^2\right]^{1/2} + \left[d_o^2 - d_b^2\right]^{1/2} - 2C \sin\psi}{2}$$

$D_b = d_b = 3.5 \text{ cas } 20° = 3.289$

$Z = \left[3.75^2 - 3.289^2\right]^{1/2} - 3.5 \times .342$

$Z = 0.6043 \qquad X_{max} = Z/2 = 0.30215$

$$R = \frac{(R_p \sin\psi + X)(R_p \sin\psi - X)}{2Rp) \sin\psi}$$

$$R = \frac{(1.75 \times .342 + .302)(1.75 \times .342 - .302)}{3.5 \times .342} = \frac{.9 \times .3}{1.2}$$

$R = 0.2255$

$U_1 = \omega R_1 \qquad U_2 = \omega R_2$

$$U_1 = \frac{\pi\, 5000}{30} \times .9 = 470 \text{ in/sec}$$

$$U_2 = \frac{\pi\, 5000}{30} \times .3 = 157 \text{ in/sec}$$

$U_1 + U_2 = 627 \text{ in/sec}$

$$\frac{h_{min}}{R} = 1.18 \left(\frac{2000}{33\times10^6 \times .2255}\right)^{-.091} \left(\frac{4.38 \times .4 \times 10^{-11} \times 627)}{.2255}\right)^{.727}$$

$$\frac{h_{min}}{R} = 12 \times 10^{-6}$$

$h_{min} = 2.7 \times 10^{-6}$

$\sigma = (12^2 + 12^2)^{1/2} = 17$

$\Lambda = \frac{h}{\sigma} = \frac{2.7}{17} = 0.16$

CONCLUDING REMARKS

The main function in the lubrication of gearing is to prevent the scoring and fatigue failure of the gear contact surfaces. Much can be done in the early stages of design of gear systems to accomplish these goals.

1. The designer should consider tip relief as an aid to improving load capacity.

2. He should also weigh the cost of improved surface finish for better load capacity against other factors.

3. In gear applications requiring high speed and/or loads special care should be given to the location and application of the lubricant for best results.

4. An analysis should be conducted to determine the EHD film thickness with care given to the worst operating conditions of temperature, speed and load. This analysis will aid in the selection of the lubricant that will give best results. It should also tell the designer if an extreme pressure additive is needed to prevent scoring.

5. In selecting an extreme pressure additive the designer should be aware of the temperature, speed and loads expected in the system.

6. Finally, because there is much that still is unknown about the lubrication of concentrated contacts a test program should be included in any new gear design program to assure successful operation of the system.

REFERENCES

1. Wellauer, E. S.: Discussion at the University of Wisconsin Gear Design Seminar, November 1968. (Unpublished).

2. Borsoff, V. A.: On the Mechanism of Gear Lubrication. J. Basic Eng., vol. 81, no. 1, March 1959, pp. 79-93.

3. Seireg, A, and Conry, T.: Optimum Design of Gear Systems for Surface Durability. ASLE Transactions, vol. 11, no. 4, October 1968, pp. 321-329.

4. McCain, J. W., and Alsandor E.: Analytical Aspects of Gear Lubrication on the Disengaging Seal. ASLE Transactions, vol. 9, no. 2, April 1966, pp. 202-211.

5. Godfrey, D.: Boundary Lubrication. Interdisciplinary Approach to Friction and Wear, NASA SP-181, 1968, pp. 335-384.

6. Fein, R. S.: Chemistry in Concentrated Conjunction Lubrication. NASA Symposium on Interdisciplinary Approach to the Lubrication of Concentrated Contacts, Vol. 2, July 1969.

7. Fein, R. S., and Kreutz, K. L.: Discussion to Reference 5, pp. 358-376.

8. Bowden, F. P. and Tabor, D.: The Friction and Lubrication of Solids. Vol. 2, Clarendon Press, Oxford, 1964, p. 365.

9. Borsoff, V. A.: Fundamentals of Gear Lubrication. Annual Rep., Shell Development Co., June 1955. (Work under Contract No. a(s) 53-356-c).

10. Borsoff, V. A. and Lulwack R.: Fundamentals of Gear Lubrication. Final Rep., Shell Development Co., June 1957. (Work under Contract No. a(s) 53-356-c).

11. Horlick, E. J. and O'D. Thomas, D. E.: Recent Experience in the Lubrication of Naval Gearing. Gear Lubrication Symposium, Institute of Petroleum, 1966.

12. Boner, C. J.: Gear and Transmission Lubricant. Reinhold Pub. Co., 1964.

13. Research Committee on Lubrication: Viscosity and Density of Over 40 Fluids at Pressures to 152,000 psi and Temperatures to 425° F. ASME, 1953.

14. Foord, C. A.; Hammann, W. C.; and Cameron, A.: Evaluation of Lubricants Using Optical Elastohydrodynamics. ASLE Transactions, vol. 11, no. 1, January 1968, pp. 31-43.

15. Sibley, L. B., and Orcutt, F. K.: Elasto-Hydrodynamic Lubrication of Rolling-Contact Surfaces. ASLE Transactions, vol. 4, no. 2, November 1961, pp. 234-249.

16. Crook, A. W.: The Lubrication of Rollers — I. Phil. Trans. Roy. Soc. (London), ser. A, vol. 250, 1957-1958, pp. 387-409.

17. Dyson, A.; Naylor, H.: and Wilson, A. R.: The Measurement of Oil-Film Thickness in Elastohydrodynamic Contacts. Elastohydrodynamic Lubrication, Mechanical Engineers, vol. 180, pt. 3B, 1965.

18. Naylor, H.: The Rheological Behavior of Lubricants. NASA Symposium on Interdisciplinary Approach to the Lubrication of Concentrated Contacts, vol. 1, July 1969.

19. Allen, C. W.; Townsend, D. P.; and Zaretsky, E. V.: Elastohydrodynamic Lubrication of a Spinning Ball in a Nonconforming Groove. J. Lubr. Tech., vol. 92, no. 1, January 1970, pp. 89-96.

20. Townsend, Dennis P. and Zaretsky, Erwin V.: Effects of Antiwear and Extreme-pressure Additives in a Synthetic Paraffinic Lubricant on Ball Spinning Torque. NASA TN D-5820, 1970.

21. Zaretsky, Erwin V. and Anderson, William J.: How to Use What We Know About EHD Lubrication. Machine Design, vol. 40, no. 26, November 7, 1968, pp. 167-173.

22. Grubin, A. N. and Venogradov, I. E.: Investigation of the Contact of Machine Components. Book 30, Central Scientific Research Institute for Technology and Mechanical Engineering (TSNI TMASH), Moscow, 1949.

23. Zaretsky, Erwin V.; Anderson, William J. and Bamberger, Eric N.: Rolling-Element Bearing Life From 400° to 600° F. NASA TN D-5002, 1969.

24. Shipley, E. E.: Gear Failure. Machine Design, vol. 39, no. 28, December 7, 1969, pp. 152-162.

TABLE I. - GEAR OIL FORMULATIONS WHICH SATISFY CONDITIONS OF HIGH-SPEED, LOW-TORQUE AND LOW-SPEED, HIGH-TORQUE (REF. 12)

	Wt. per cent	Wt. per cent	Wt. per cent
Solvent B.S. vis. 600 Redwood I at 140° F	58.0	----	-----
Solvent oil-150 Redwood I at 140° F	25.0	----	-----
Solvent oil-65 Redwood I at 140° F	8.0	----	-----
Chlorinated paraffin wax-40% Cl	3.7	----	-----
Dibenzyl disulfide	2.8	----	-----
Di-isopropyl phosphite	1.4	----	-----
Oil concentrate 85% of zinc salts of dihexyl and di-isopropyl phosphorodithioic acids	.5	----	-----
Oil concentrate 40% basic calcium petroleum sulfonate	.5	----	-----
Polymethacrylate type pour depressant	.1	----	-----
Additive A	----	6.9	-----
Zinc dihexyl dithiophosphate	----	5.5	-----
Oil, 90 V.I., 1094 vis. SUS at100° F	----	87.6	-----
Zinc di-(4-methyl-2-pentyl) phosphorodithioate	----	----	4.4
Di-benzyl polysulfides	----	----	2.05
SAE 90 grade gear oil	----	----	93.55

TABLE II. - EP GEAR OILS CONTAINING LEAD COMPOUNDS (REF. 12)

Composition	A	B	C	D
	Per cent by weight			
Lead naphthenate	8	7	----	----
Sulfochlorinated sperm oil	8	7	----	----
Chlorinated paraffin wax	2.5	----	----	----
Sulfurized sperm oil	4	3	----	----
"SCL"	----	----	28.5	28.5
Diphenylamine	----	.3	----	----
SAE 90 grade oil	77.5	----	----	----
500 at 100 solvent oil	----	23.0	----	----
200 solvent bright stock	----	66.7	----	41.5
200 at 210 black oil	----	----	46.0	----
100 at 100 Arkansas oil	----	----	25.5	----
400 at 100 solvent oil	----	----	----	30.0

TABLE III. - TURBOJET LUBRICANT (REF. 12)

Ingredient	Purpose	Per cent
Dodecylamine dodecyl acid phosphate	EP agent	0.12
Dodecyl dihydrogen phosphate	EP agent	.08
Tricresyl phosphate	Anti-wear agent	2.0
Phenyl alpha naphthylamine	Oxidation inhibtor	1.0
Quinizarin	Metal deactivator	.02
Dimethyl silicon	Anti-foam agent	.001
Fluid		96.78

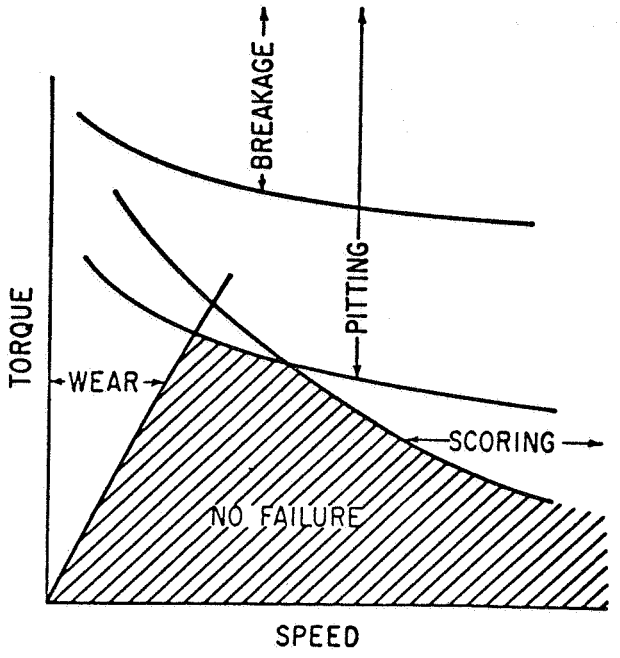

Figure 1. - Gear performance limits (ref. 1).

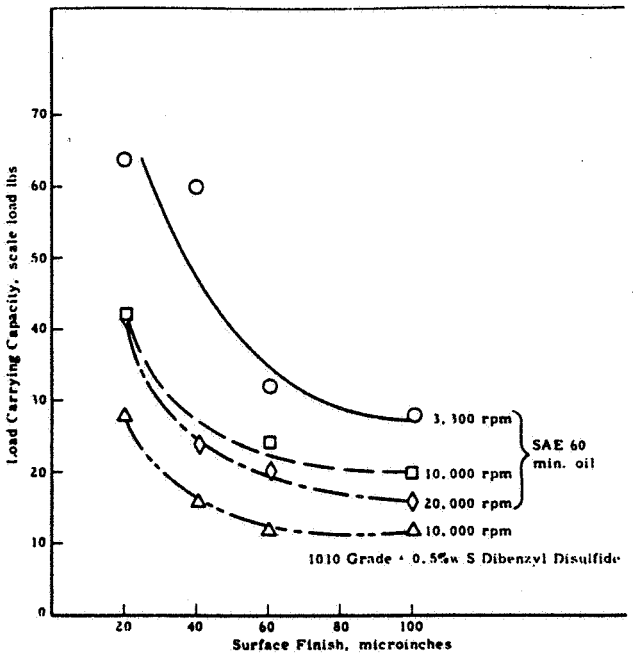

Figure 2. - Load carrying capacity versus surface finish (ref. 2).

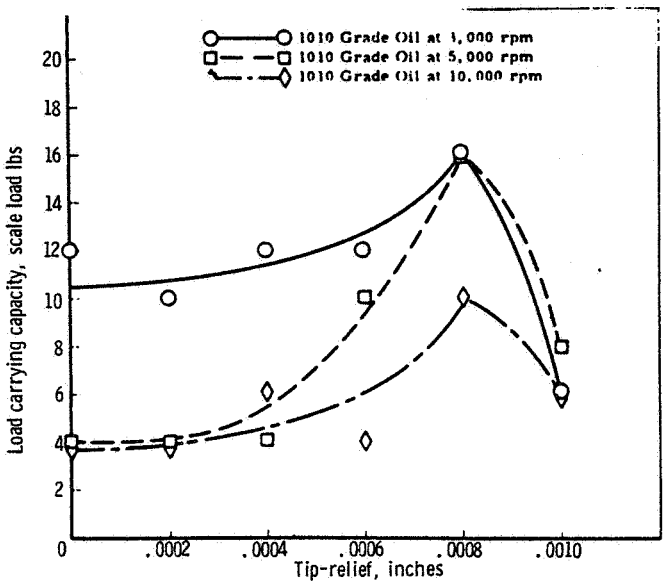

Figure 3. - Effect of tip-relief on load carrying capacity (ref. 2).

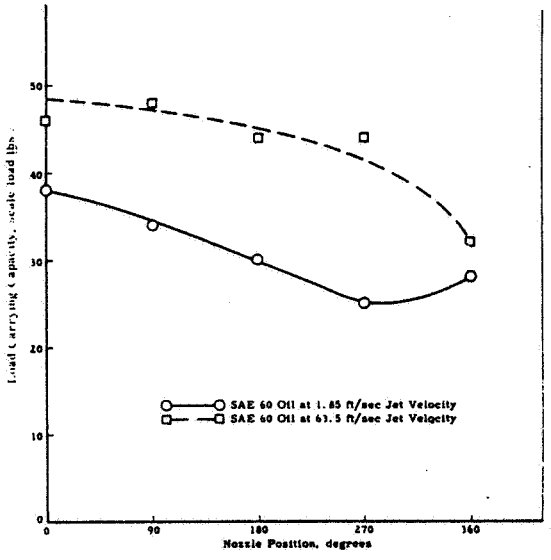

Figure 4. - Effect of jet velocity and point of application on load carrying capacity (ref. 2).

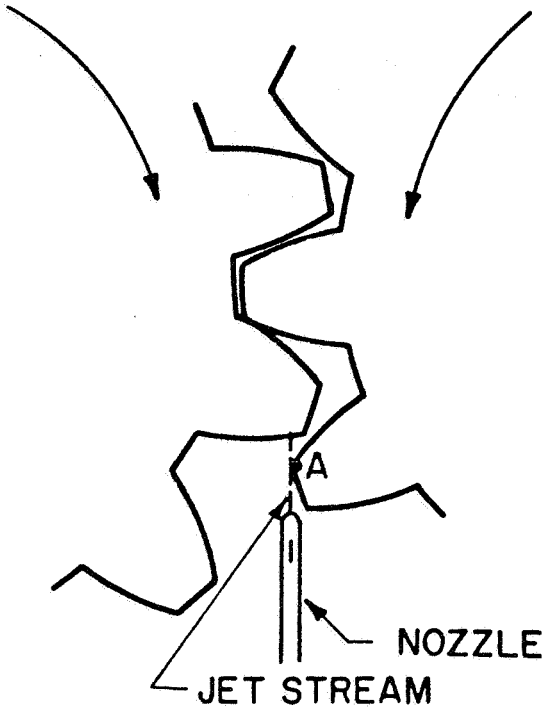

Figure 5. - Schematic of vertically oriented jet showing position for maximum oil penetration (ref. 3).

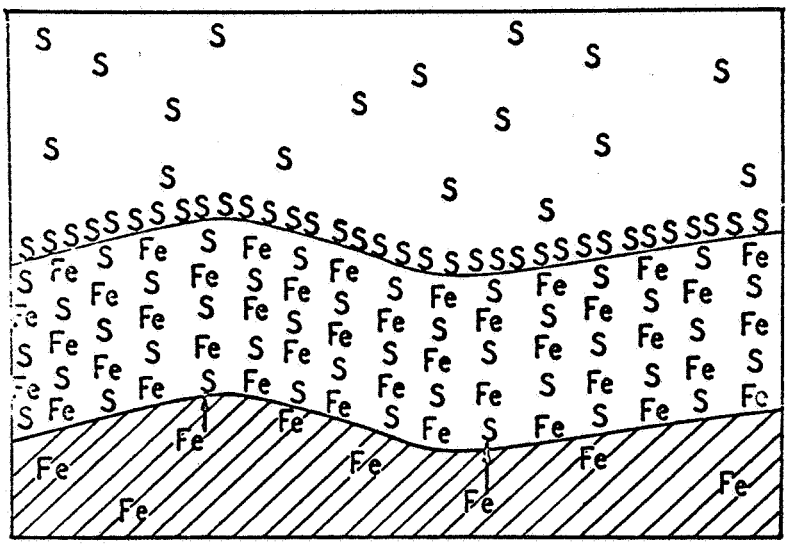

Figure 6. - Schematic representation of an inorganic film formed by reaction of sulfur with iron to form iron sulfide (ref. 5).

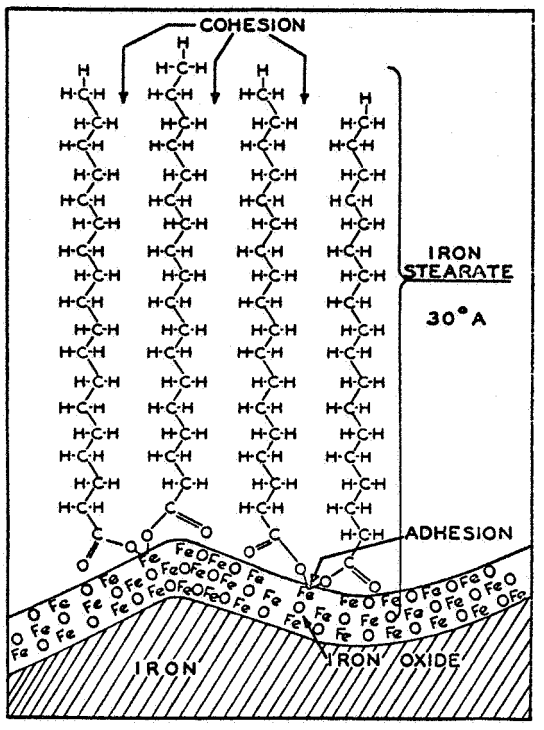

Figure 7. - Schematic diagram representing the chemisorption of stearic acid on an iron surface to form a monolayer of iron stearate, a soap (ref. 5).

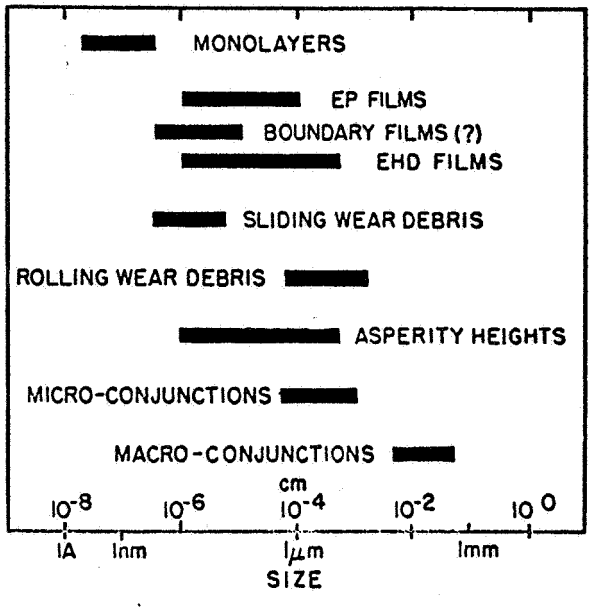

Figure 8. - Sizes pertinent to concentrated conjunction lubrication (ref. 6).

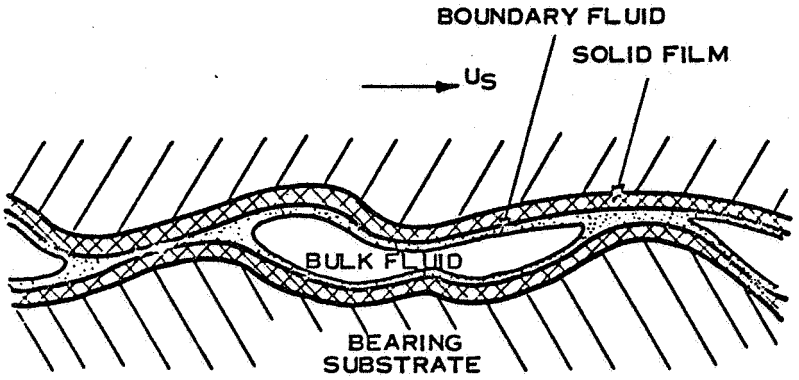

Figure 9. - Generalized MICRO-EHD model (ref. 7).

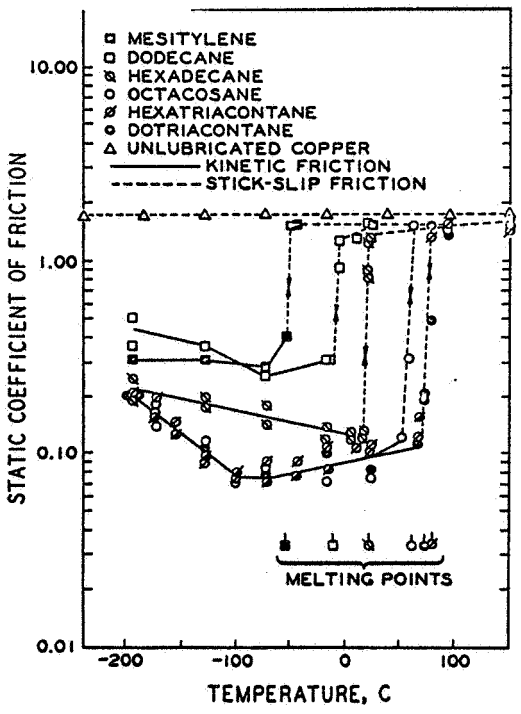

Figure 10. - Variation in friction with temperature for copper pairs lubricated with hydrocarbons in dry helium (ref. 5).

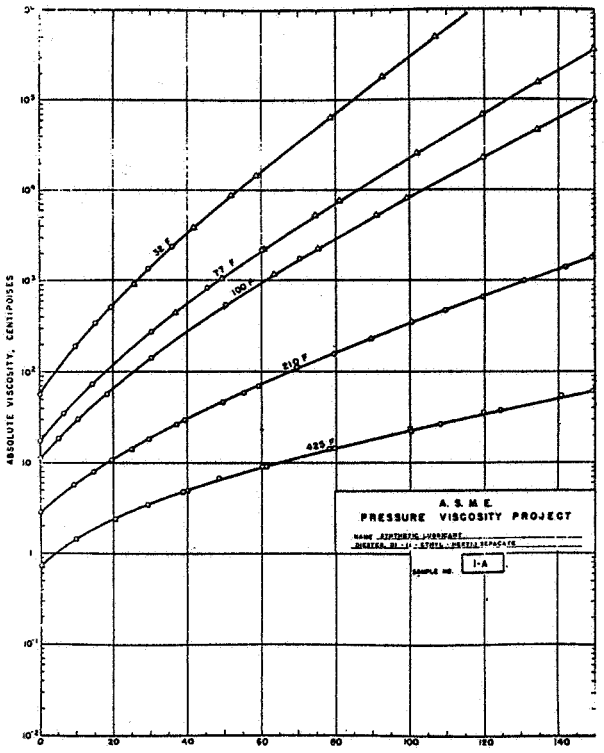

Figure 11. - (ref. 13).

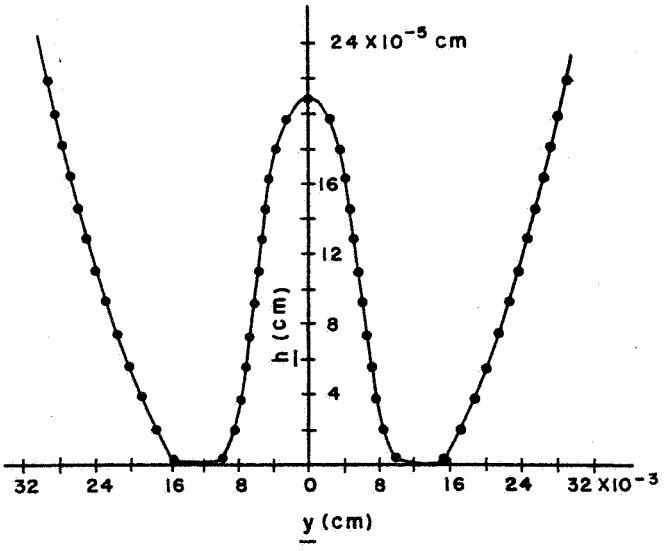

Figure 12. - Cross section through a squeeze film dimple (ref. 14).

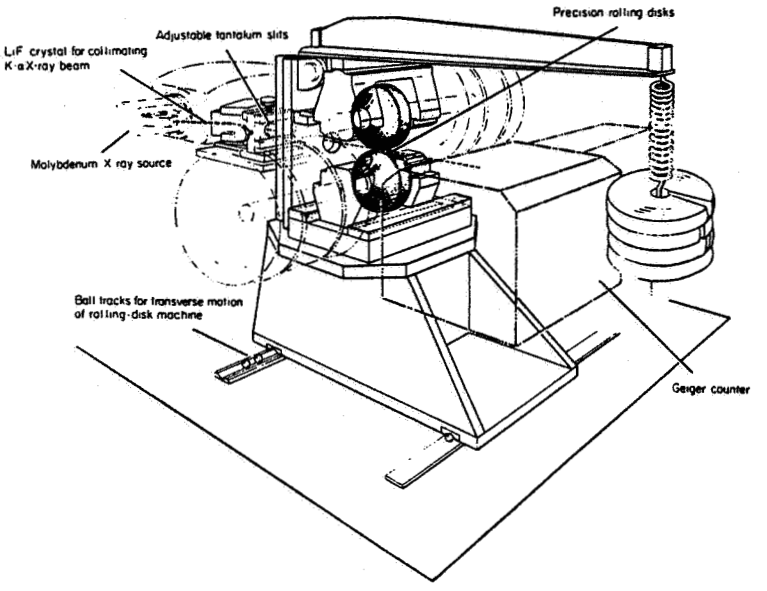

Figure 13. - Sketch of precision rolling-disk machine and X-ray system for rolling-contact-lubrication experiments (ref. 15).

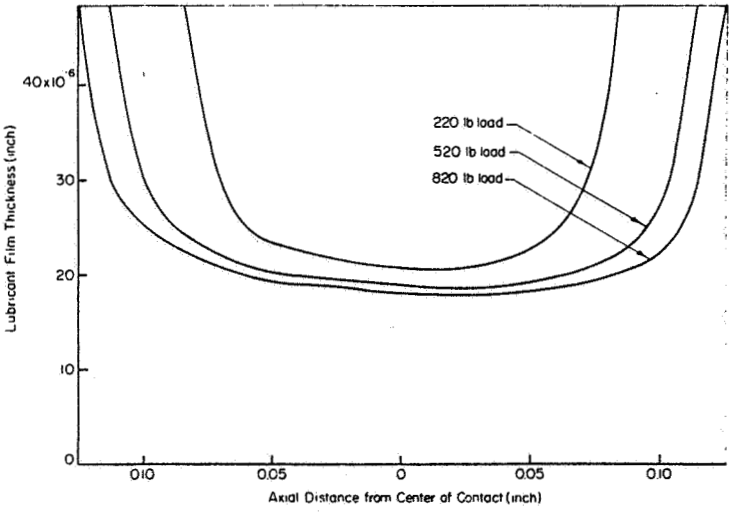

Figure 14. - Effect of lead on film shape between rollers. 15 cs white mineral oil (128° F roller temperature), 2600 fpm rolling speed, smooth curves have been drawn through profile traces (ref. 15).

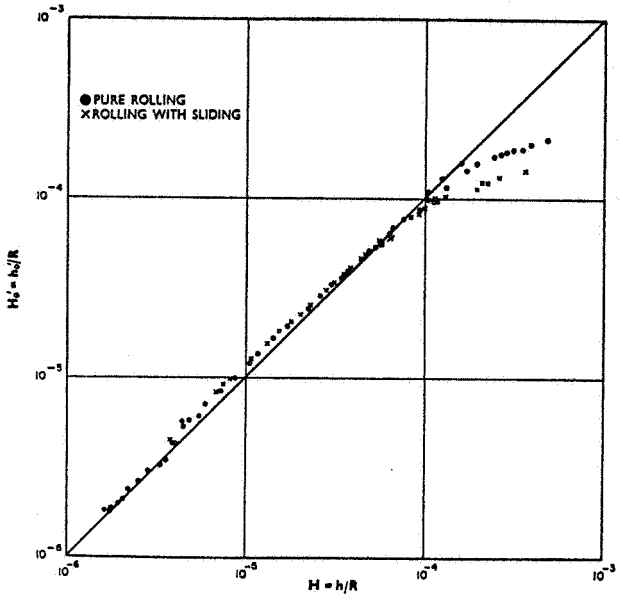

Figure 15. - Lubricant B: comparison of measured non-dimensional oil-film thickness $H_0' = h_0'/R$ with predicted values $H = h/R$ (ref. 17).

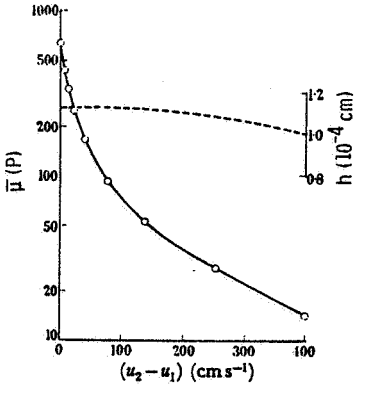

Figure 16. - The effective oil viscosity within the pressure zone ($\bar{\mu}$) as a function of sliding speed. Load 7.4×10^7 dyn cm^{-1}; —o—, $\bar{\mu}$ (logarithmic scale); ——, h (linear scale) (ref. 16).

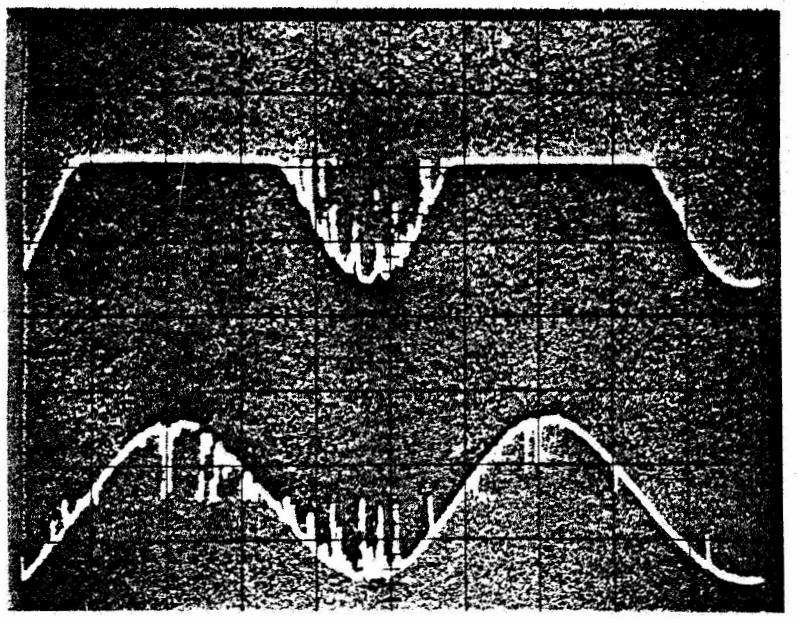

Figure 17. - Photo of 400 hertz trace of conductivity method of EHD film measurement.

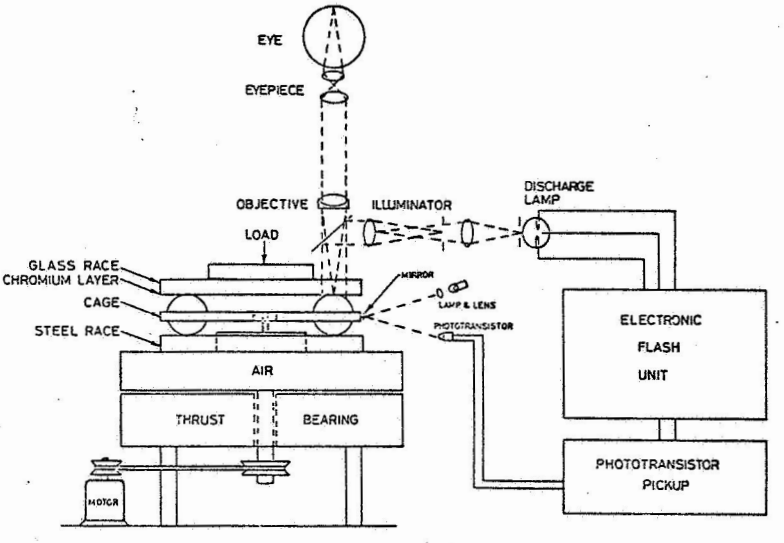

Figure 18. - Schematic diagram of optical EHD apparatus (ref. 14).

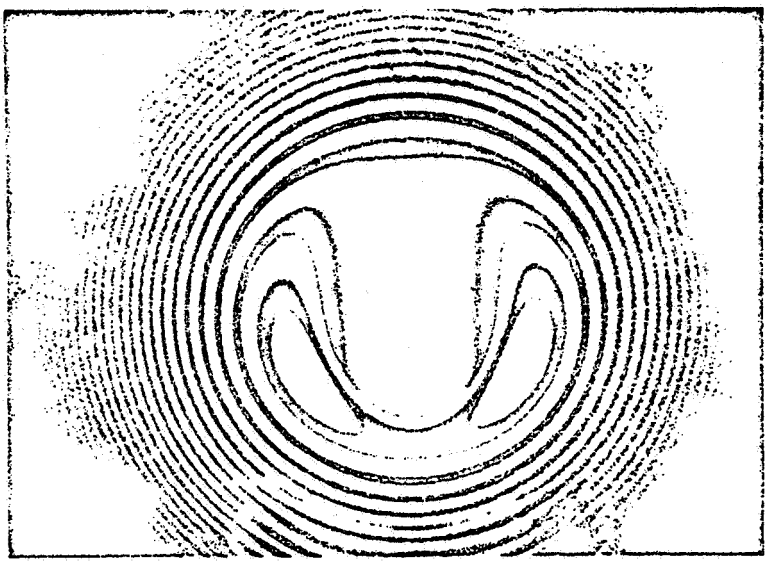

Figure 19. - Photo of optical EHD image as seen through eyepiece (ref. 14).

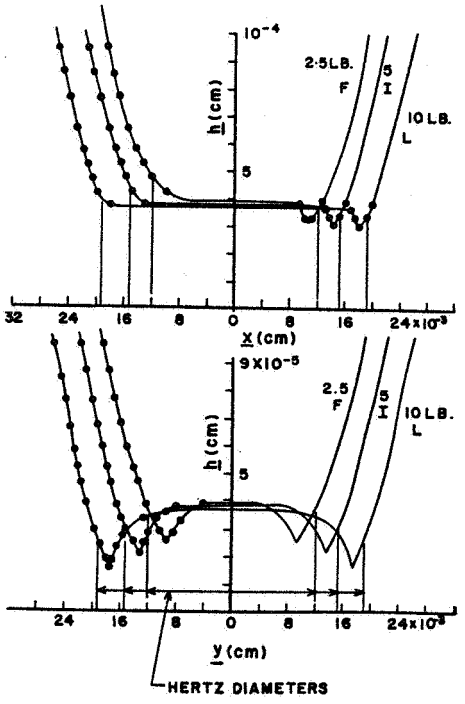

Figure 20. - Oil film profiles at different loads (ref. 14).

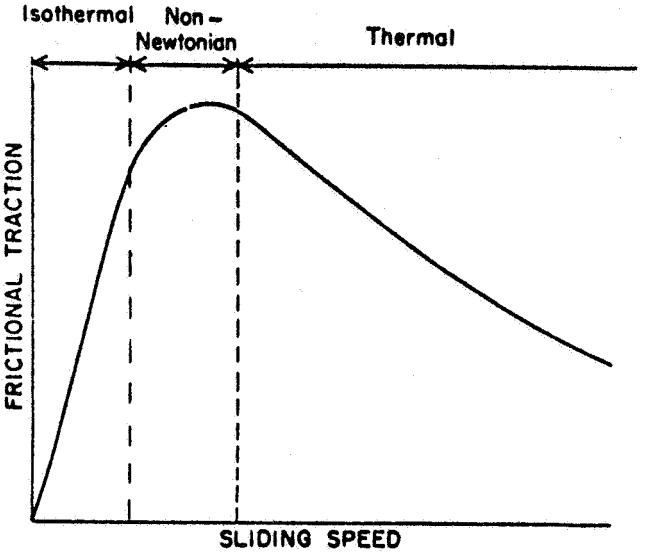

Figure 21. - Plot of friction against sliding speed (ref. 18).

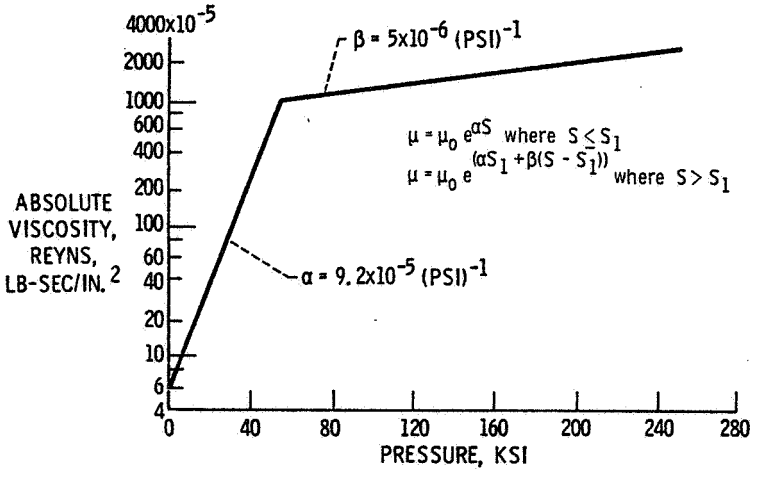

Figure 22. - Theoretical pressure-viscosity relation for synthetic paraffinic oil at 83° F (ref. 20).

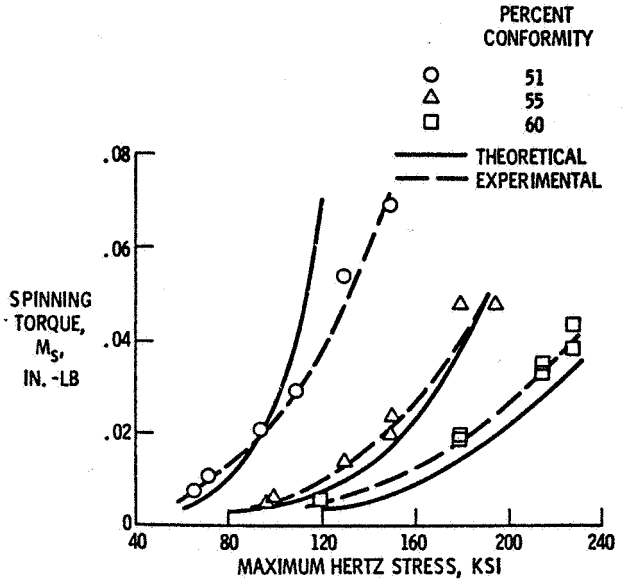

Figure 23. - Spinning torque as a function of maximum Hertz stress. Ball-oil conformity, 51, 55, and 60 percent; lubricant, synthetic paraffinic oil; pinning speed, 1050 rpm; room temperature (no heat added) (ref. 20).

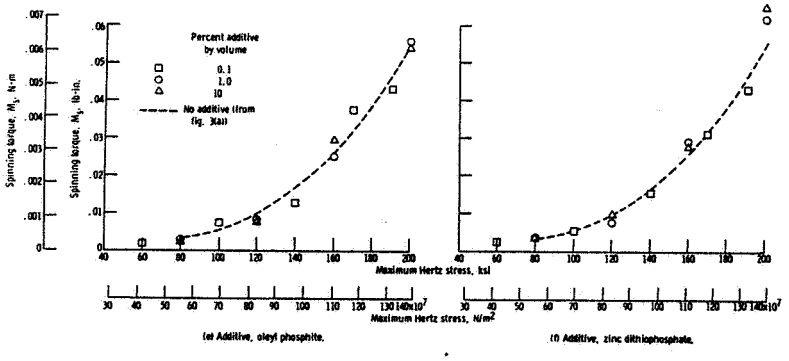

Figure 24. - Spinning torque as a function of maximum Hertz stress for synthetic paraffinic lubricant with several additives (ref. 20).

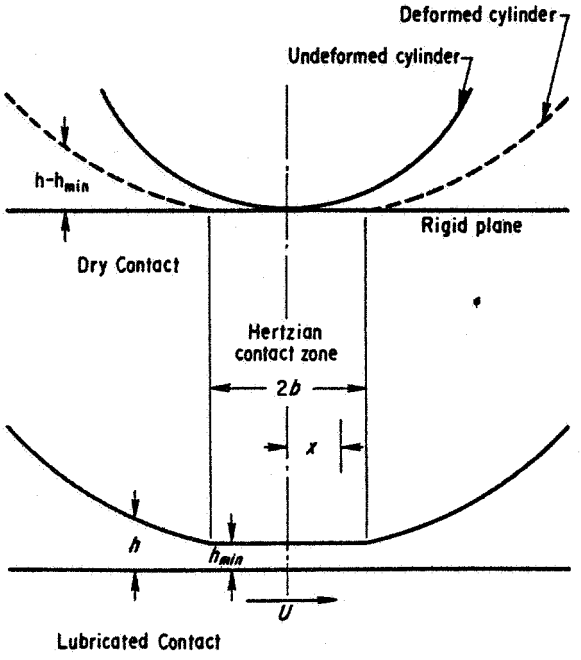

Figure 25. - Grubin's model for an EHD contact (ref. 22).

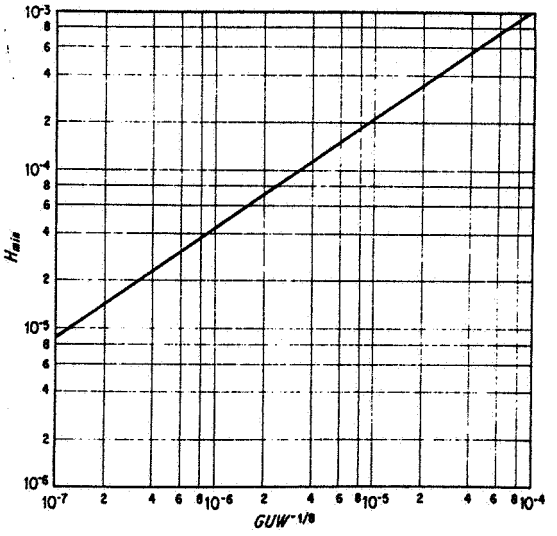

Figure 26. - Dimensionless film thickness parameter as a function of EHD parameters (ref. 21).

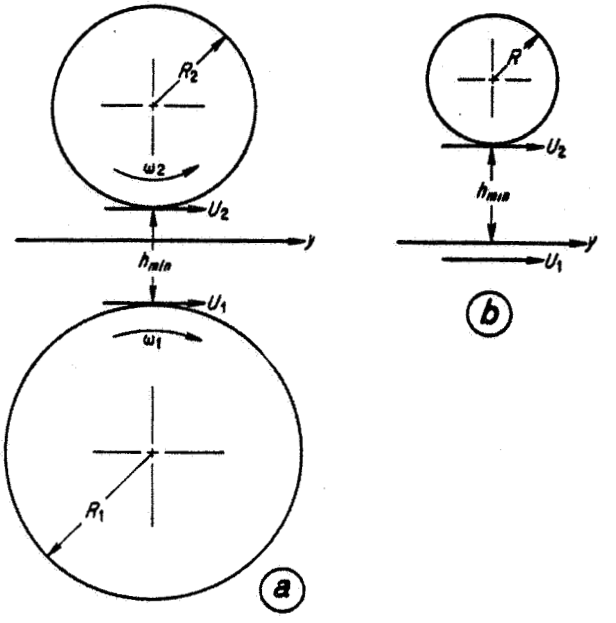

Figure 27. - Relationship between two cylinders with a lubricant film between them, a, and model of an equivalent cylinder, b (ref. 21).

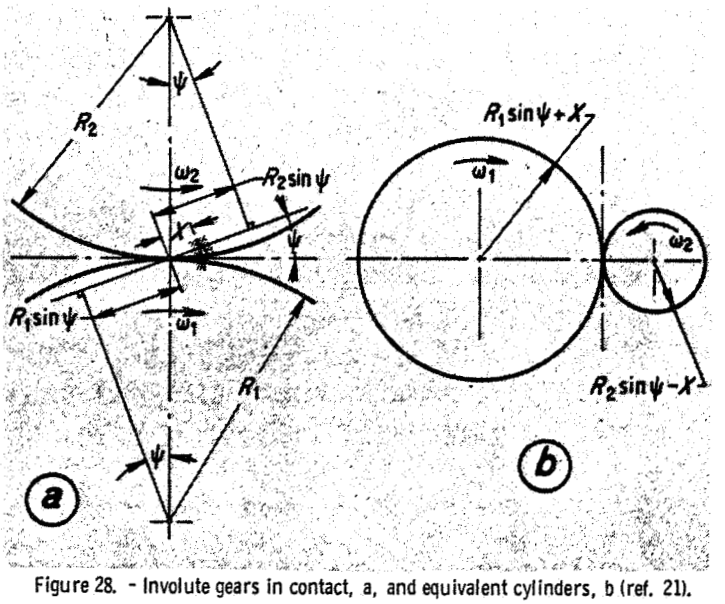

Figure 28. - Involute gears in contact, a, and equivalent cylinders, b (ref. 21).

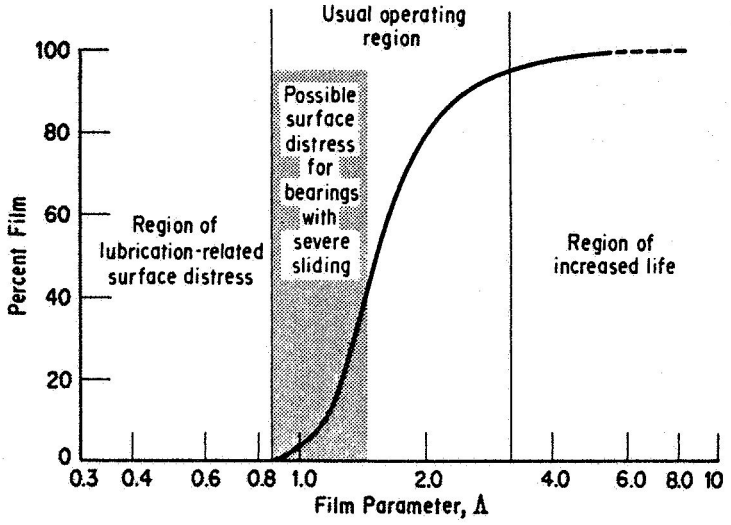

Figure 29. - Percent film as a function of film parameter (ref. 21). (Courtesy of SKF Industries Inc.)

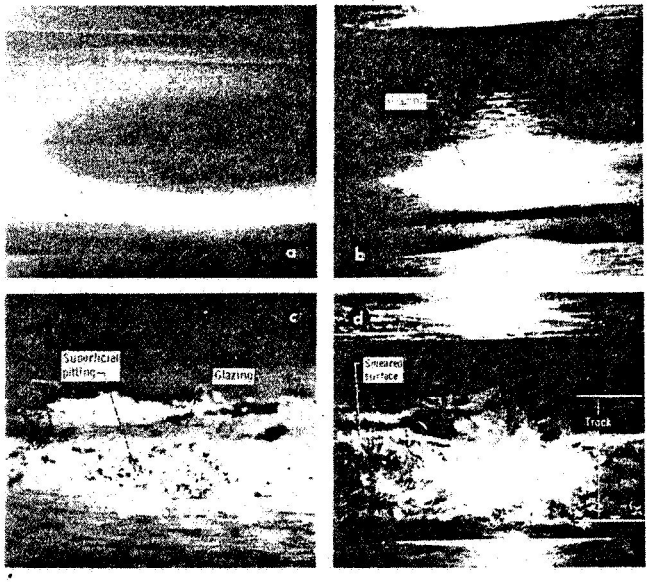

Figure 30. - Effect of EHD lubrication on surface damage to bearing races. Full EHD film results in normal race appearance, a. Marginal EHD film results in race glazing, b; glazing and superficial pitting, c; and gross plastic deformation or smearing, d.

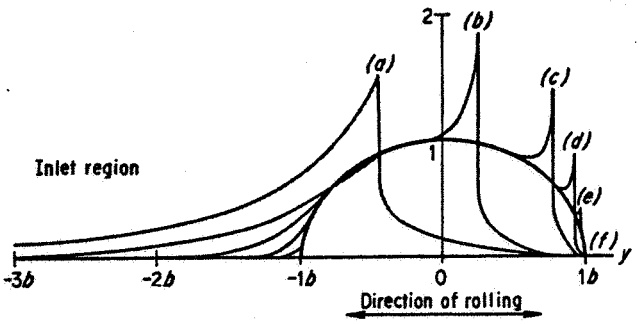

$W = 3 \times 10^{-5}$, $G = 5000$
$U = (a)\ 10^{-9}$, $(b)\ 10^{-10}$, $(c)\ 10^{-11}$, $(d)\ 10^{-12}$, $(e)\ 10^{-13}$, $(f)\ 0$ (dry)
$U/W^2 = (a)$ 1.1, (b) 0.11, (c) 0.011, (d) 0.0011, (e) 0.00011

Figure 31. - Theoretical pressure distributions between lubricated rolling cylinders. As velocity increases, pressure spike shifts toward leading edge of contact (ref. 21).

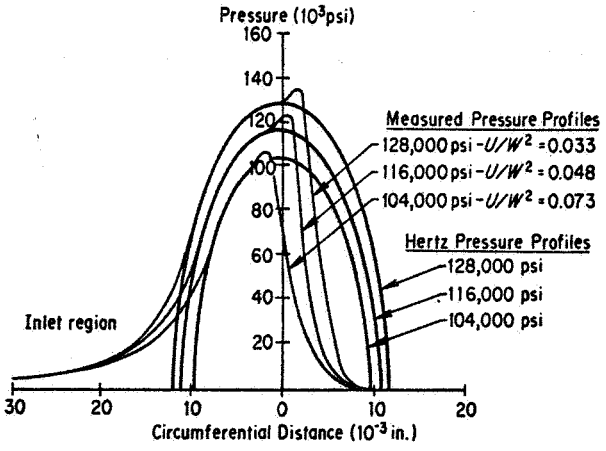

Figure 32. - Comparison of calculated Hertz pressure profiles and measured profiles between cylindrical discs with polyphenyl ether lubricant (ref. 21).

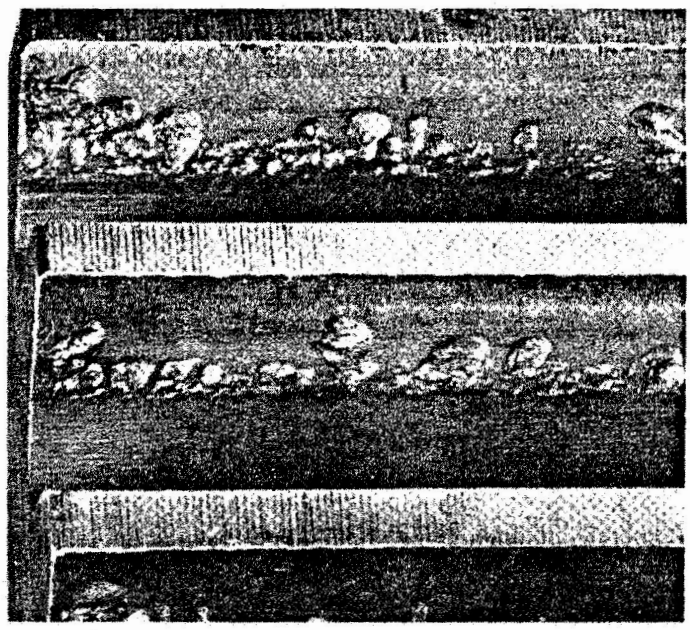

Figure 33. - Destructive pitting: Heavy pitting has taken place, predominantly in the dedendum region (ref. 24).